Redox Biology 2 (2014) 921–928

Contents lists available at ScienceDirect

Redox Biology

journal homepage: www.elsevier.com/locate/redox

Research Paper

Oxidative damage in the gastrocnemius of patients with peripheral artery disease is myofiber type selective

Panagiotis Koutakis [a,1], Dustin J. Weiss [a,1], Dimitrios Miserlis [a], Valerie K. Shostrom [b], Evlampia Papoutsi [a], Duy M. Ha [a], Lauren A. Carpenter [a], Rodney D. McComb [c], George P. Casale [a,*,2], Iraklis I. Pipinos [a,d,*,2]

[a] Department of Surgery, University of Nebraska Medical Center, Omaha, NE, United States
[b] Department of Biostatistics, University of Nebraska Medical Center, Omaha, NE, United States
[c] Department of Pathology and Microbiology, University of Nebraska Medical Center, Omaha, NE, United States
[d] Department of Surgery and VA Research Service, VA Nebraska-Western Iowa Health Care System, Omaha, NE, United States

ARTICLE INFO

Article history:
Received 29 June 2014
Accepted 7 July 2014
Available online 19 July 2014

Keywords:
carbonyl groups
oxidative damage
Fontaine Stage

ABSTRACT

Background: Peripheral artery disease (PAD), a manifestation of systemic atherosclerosis that produces blockages in the arteries supplying the legs, affects approximately 5% of Americans. We have previously, demonstrated that a myopathy characterized by myofiber oxidative damage and degeneration is central to PAD pathophysiology.
Objectives: In this study, we hypothesized that increased oxidative damage in the myofibers of the gastrocnemius of PAD patients is myofiber-type selective and correlates with reduced myofiber size.
Methods: Needle biopsies were taken from the gastrocnemius of 53 PAD patients (28 with early PAD and 25 with advanced PAD) and 25 controls. Carbonyl groups (marker of oxidative damage), were quantified in myofibers of slide-mounted tissue, by quantitative fluorescence microscopy. Myofiber cross-sectional area was determined from sarcolemma labeled with wheat germ agglutinin. The tissues were also labeled for myosin I and II, permitting quantification of oxidative damage to and relative frequency of the different myofiber Types (Type I, Type II and mixed Type I/II myofibers). We compared PAD patients in early ($N=28$) *vs.* advanced ($N=25$) disease stage for selective, myofiber oxidative damage and altered morphometrics.
Results: The carbonyl content of gastrocnemius myofibers was higher in PAD patients compared to control subjects, for all three myofiber types ($p<0.05$). In PAD patients carbonyl content was higher ($p<0.05$) in Type II and I/II fibers compared to Type I fibers. Furthermore, the relative frequency and cross-sectional area of Type II fibers were lower, while the relative frequencies and cross-sectional area of Type I and Type I/II fibers were higher, in PAD compared to control gastrocnemius ($p<0.05$). Lastly, the type II-selective oxidative damage increased and myofiber size decreased as the disease progressed from the early to advanced stage.
Conclusions: Our data confirm increased myofiber oxidative damage and reduced myofiber size in PAD gastrocnemius and demonstrate that the damage is selective for type II myofibers and is worse in the most advanced stage of PAD.

Introduction

Peripheral arterial disease (PAD), is characterized by the formation of atherosclerotic plaques that limit blood flow to the legs, and affects approximately 5% of the general population, with the prevalence increasing to 15–20% in persons over 70 years [1]. PAD is commonly divided in four clinical stages [1]. In the early stage of PAD, the patients experience no symptoms. This stage is defined as Stage I (asymptomatic PAD) according to the Fontaine classification system. By far, the most common clinical manifestation of

* Correspondence to: Department of Surgery, 983280 Nebraska Medical Center, Omaha, NE 68198, United States.
E-mail addresses: gpcasale@unmc.edu (G.P. Casale), ipipinos@unmc.edu (I.I. Pipinos).
[1] Co-first authors.
[2] Co-senior authors.

http://dx.doi.org/10.1016/j.redox.2014.07.002

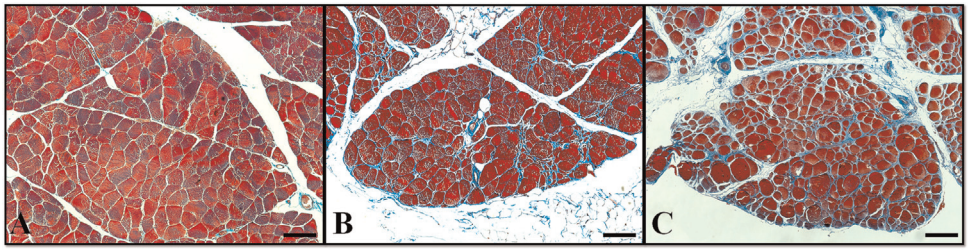

Fig. 1. Myopathy in PAD limbs is easily demonstrated. Control skeletal muscle (A) and ischemic muscle from age- and sex-matched PAD patients with early (B) and late stage (C) disease were stained with Masson trichrome and images were captured under bright-field conditions with a 10× objective. Control muscle (A) exhibits polygonal myofibers of uniform shape and size and thin endomysium and perimysium. Myofiber shape and size are less uniform in early stage PAD muscle (B). The specimen includes large, swollen fibers, irregularly-shaped microfibers and thickened, collagenous endomysium and perimysium. Most myofibers of late stage muscle (C) are irregular in shape and size and include many large, rounded and swollen fibers and many small, irregularly shaped fibers. There is extensive replacement of myofibers with fibrous tissue. The black bars represent a length of 100 μm.

symptomatic PAD is claudication (*i.e.*, Fontaine Stage II), a severe functional limitation identified as gait dysfunction and walking-induced leg muscle pain relieved by rest. In its less common advanced stages, symptomatic PAD becomes limb-threatening and patients have foot pain at rest (*i.e.*, Fontaine Stage III) or more commonly non-healing ulcers and necrosis/gangrene (*i.e.*, Fontaine Stage IV).

Previous studies, have documented a myopathy in the PAD muscle that is characterized by defective mitochondrial bioenergetics, oxidative stress and abnormal skeletal muscle histomorphology and function (Fig. 1) [2–10]. Our group has previously shown the central importance of oxidative damage in the pathophysiology of PAD myopathy demonstrating a significant increase in oxidative damage in PAD muscle and its myofibers compared to controls. At the myofiber level, we found that the levels of oxidative damage in PAD increase as the hemodynamics of the blood flow to the leg worsen and as the disease advances from Fontaine stage II to stage III and stage IV [10]. Furthermore, we have shown that oxidative damage is not a homogeneously diffuse process but varies from myofiber to myofiber in the affected muscles and that the more atrophic myofibers have higher levels of oxidative damage [10]. Mechanistically, it is not known whether oxidative damage in PAD limbs is selective for a specific subpopulation of myofibers and whether certain characteristics of myofibers may make them more sensitive or prone to oxidative damage.

The myofibers of human muscles belong to three classes differentiated on the basis of myosin heavy chain phenotype and differing on the basis of their speed of contraction and predominant type of energy metabolism [11]. Type I (slow twitch) fibers are characterized by higher mitochondrial content and more oxidative energy metabolism. Type II (fast twitch) fibers have a lower mitochondrial content and greater dependence on glycolysis. Mixed (Type I/II) fibers are intermediate in mitochondrial content and energy metabolism and are transitioning between Type I and Type II fibers. Other groups have previously evaluated the different types of myofibers in the gastrocnemius of ischemic limbs of PAD patients. Their findings have demonstrated a tendency for selective loss of Type II fibers relative to Type I fibers and a significant decrease in the average cross sectional area of individual Type II fibers [3,9]. Considering the possibility that the finding of selective loss of Type II fibers is related to increased oxidative damage in this type of fibers we hypothesized that increased oxidative damage in ischemic muscle of PAD patients is myofiber type selective and correlates with reduced myofiber size. We also hypothesized that oxidative stress and its myofiber type selectivity, will increase with advancing disease stage from stage II to stage IV.

Materials and methods

Human subjects

The experimental protocol was approved by the Institutional Review Board, of the VA, Nebraska-Western Iowa and University of Nebraska Medical Centers, and all subjects gave informed consent. We recruited 53 patients evaluated for symptomatic PAD (Table 1). Twenty eight patients presented with claudication (PAD-II; Fontaine Stage II) and twenty five presented with tissue loss (PAD-IV;

Table 1
Baseline characteristics of PAD and control subjects.

	Control subjects	PAD patients			
		Combined	PAD-II	PAD-IV	*p*-Value*
Number of subjects	25	53	28	25	_
Mean age (years)	62.7 ± 2.1	64.7 ± 1.0	62.6 ± 1.7	67.0 ± 1.6	0.340
Ankle brachial index	1.08 ± 0.02	0.40 ± 0.04	0.53 ± 0.04	0.25 ± 0.04	< 0.001
Gender % (male/female)	80/20	94.3/5.7	92.9/7.1	96/4	0.102
Smoking	28.00%	67.9%	67.90%	68.00%	0.001
Coronary artery disease	24.0%	45.3%	39.30%	52.00%	0.085
Obesity	44.0%	22.6%	17.90%	28.00%	0.066
Dyslipidemia	52.0%	64.2%	71.40%	56.00%	0.331
Type 1 diabetes mellitus	32.0%	49.1%	32.10%	56.00%	0.222
Family history of PAD	12.0%	15.1%	21.40%	8.00%	0.714
Hypertension	72.0%	77.4%	75.00%	80.00%	0.778

Note: Continuous variables are presented as mean ± S.E.M.

* *p* Values are for differences between control subjects and PAD patients "combined"; chi-square or Fisher's exact tests were used for categorical variables; independent *t* test was used for continuous variables.

Fontaine Stage IV). For every patient, the diagnosis of PAD was established on the basis of medical history, physical examination, significantly decreased ankle-brachial index (ABI) and computerized or standard arteriography. We recruited twenty five patients with normal blood flow to their lower limbs, undergoing lower extremity operations for indications other than PAD (Table 1). These patients had no history of PAD symptoms, and all had normal lower extremity pulses at examination. All controls were selected to have normal ABIs at rest and after stress and all led sedentary lifestyles.

Muscle biopsy

Gastrocnemius samples were obtained from the anteromedial aspect of the muscle belly, 10 cm distal to the tibial tuberosity. All biopsies were obtained with a 6 mm Bergstrom needle. The samples were placed immediately into cold methacarn. After 48 h in methacarn, the specimens were transferred to cold ethanol:H_2O (50:50 v/v) and subsequently embedded in paraffin.

Quantitative fluorescence microscopy

Paraffin-embedded biopsies sectioned at 4 μm were labeled with three fluorescent reagents for identifying Type I and Type II fibers and for quantification of ROS-induced oxidative damage in myofibers. Slide specimens of gastrocnemius biopsies were deparaffinized, rehydrated, and treated with 100 mM citrate buffer (pH 6.0) at 90 °C for 15 min. For measurement of protein carbonyls [10,12], endogenous biotin was blocked and then carbonyl groups were biotinylated by treatment of slide specimens, first with 5 mM EZ-Link Hydrazide Biocytin (Thermo Scientific-Pierce Protein Research Products, Rockford, IL; #28020) in 100 mM 2-morpholinoethane sulfonic acid buffer (pH 6.5) for 1 h and then with cold 15 mM cyanoborohydride in Dulbecco's PBS for 1 h. For labeling of Type I and Type II fibers, specimens were blocked with 10% goat serum and treated with a mixture of mouse monoclonal antibody specific for Type I MHC (1 μg/mL; Sigma-Aldrich, St. Louis, MO) and a rabbit polyclonal antibody specific for Type II MHC (1 μg/mL; Abcam, Cambridge, MA). Control slides were treated with a mixture of mouse (1 μg/mL; eBioscience, San Diego, CA) and rabbit IgG (1 μg/mL; eBioscience, San Diego, CA). After overnight incubation for 12 h at 4 °C, the slides were labeled for 1 h, at room temperature, with a mixture of Alexa Fluor® 488 conjugated streptavidin (10 μg/mL; Life Technologies-Molecular Probes, Grand Island, NY), an Alexa Fluor® 555 conjugated goat anti-mouse IgG (10 μg/mL; Life Technologies-Molecular Probes) and an Alexa Fluor® 647 conjugated goat anti-rabbit IgG (10 μg/mL; Life Technologies-Molecular Probes). The conditions for all the fluorescent labels were adjusted to achieve maximal fluorescence signals required for quantitative analysis [13,14]. Subsequently, myofiber sarcolemmas were labeled for 1 h with Alexa Fluor® 350 conjugated Wheat Germ Agglutinin (10 μg/mL; Life Technologies-Molecular Probes). The specimens were mounted in ProLong Gold® anti-fade medium with DAPI (Life Technologies-Molecular Probes). Duplicate slides of each biopsy specimen were analyzed. Isotype control slides exhibited no detectable fluorescence labeling.

Image acquisition and analysis

Gray-scale (12-bit) fluorescence images (1344 × 1044) were captured with a widefield, epifluorescence microscope (Leica DMRXA2; North Central Instruments, Plymouth, MN) (10 × objective; 0.5128 μm/pixel), a B/W CCD camera (Orca ER C4742-95; Hamamatsu Photonics, Bridgewater, NJ) and HCImage Hamamatsu software (64-bit v.4.1; Hamamatsu Photonics, Bridgewater, NJ). An acquisition matrix was programed into the HCImage software to cover the whole muscle specimen area, acquiring a range of 60–150 microscopic frames per specimen yielding images of 80,640 × 62,640–201,600 × 156,600 pixels. At each location, images were collected in fluorescence channels corresponding to each fluorophore; (1) excitation at 350 nm and emission at 460 nm (Alexa Fluor 350), (2) excitation 480 nm and emission at 535 nm (Alexa Fluor 488), (3) excitation 555 nm and emission at 565 nm (Alexa Fluor 555) and (4) excitation 647 nm and emission at 670 nm (Alexa Fluor 647). The frames corresponding to each fluorophore were montaged in one large image to represent the given (whole) specimen. Image segmentation was done with a custom made Matlab algorithm (R2012a, Mathworks Inc., Natic, MA), using thresholding, edge detection, regionprops and a set of heuristics [2]. Labeled sarcolemma acquired at 460 nm provided a binary image that served as an outline for each myofiber was imposed on the images of Type I fibers acquired at 565 nm (Fig. 2) and Type II fibers acquired at 670 nm (Fig. 2) fibers. Then, images of Type I and II fibers were extracted separately as well as those labeled with both Type I/II identified as mixed fibers (Fig. 2). Subsequently, images of carbonyl groups acquired at 535 nm were extracted for each myofiber Types I, II and I/II (Fig. 2). Measurements of myofiber size, including cross-sectional area, equivalent diameter and perimeter, and myofiber shape, including roundness and solidity, were calculated for each myofiber classified as Types I, II, I/II. The methods describing how these parameters were measured have been described in detail [2]. Briefly, we calculated (1) myofiber cross-sectional area, as the number of pixels enclosed within a segmented myofiber, (2) myofiber perimeter, as the number of pixels on the boundary of the myofiber, (3) equivalent diameter, as the diameter of a circle that has the same area as the segmented myofiber region, (4) roundness, as the equivalent diameter x π divided by the perimeter of the segmented region, and (5) solidity, defined as the myofiber cross-sectional area divided by the area of a fitted convex hull. A fitted convex hull is the smallest convex polygon that can encompass the myofiber.

Statistical analyzes

Baseline characteristics between PAD patients and control subjects were compared using chi-square or Fischer's exact tests for categorical variables and independent *t*-tests for continuous variables. A one-way analysis of covariance was used to identify differences between PAD and control groups for all myofiber types adjusting for the effects of smoking status, followed by *post-hoc* analyzes with Bonferroni correction. A one-factor repeated measures design was used to identify differences among fiber types within each group, followed by *post-hoc* analyzes with Bonferroni correction. Partial bivariate correlations were used to correlate oxidative damage with myofiber morphology parameters adjusting for the effect of smoking status. All analyzes were performed using SAS statistical software version 9.3 (SAS Institute Inc., Cary, North Carolina).

Results

Subject demographics

The baseline demographic and clinical characteristics are presented in Table 1. As expected, PAD patients had significantly lower ABI values than control subjects (PAD 0.40 ± 0.04 *vs.* controls: 1.08 ± 0.02, $p < 0.001$). Smoking status was significantly higher in PAD patients compared to controls ($\chi^2 = 10.9$, $p = 0.001$). No other differences were found among the PAD patients and control subjects.

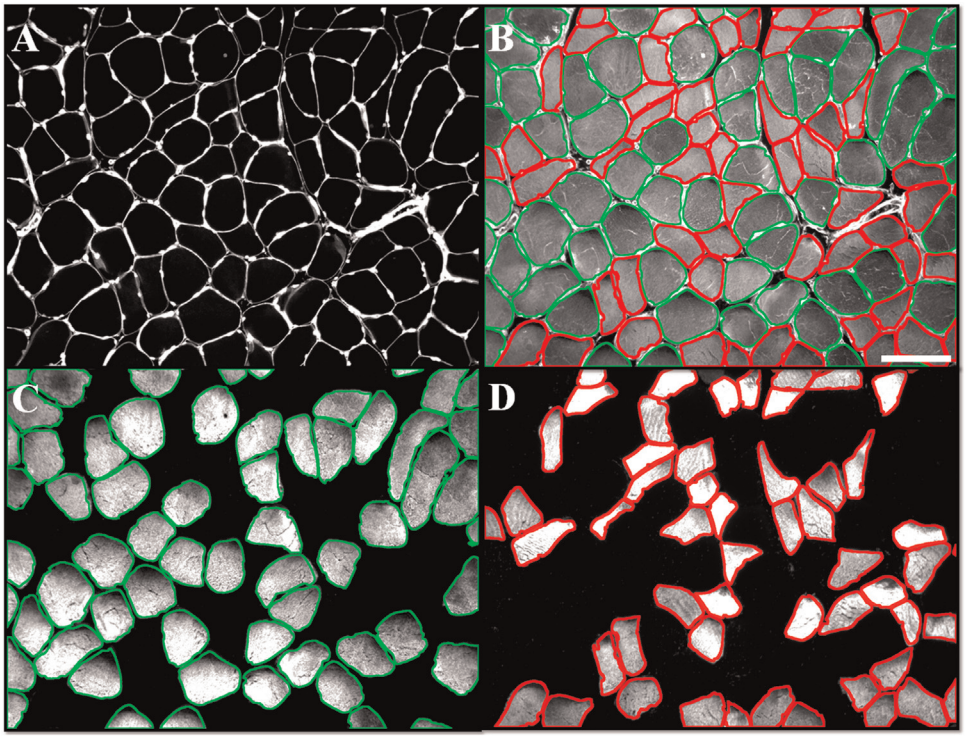

Fig. 2. Each muscle specimen was labeled for identification of nuclei (A, bright nodes along the sarcolemma), sarcolemma (A, white outlines), and Type I (C) and Type II (D) myosin heavy chain and for quantification of myofiber carbonyl content (B, gray). Sarcolemmal outlines of Type I (C, green outlines) and Type II (D, red outlines) fibers were superimposed on the carbonyl image (B), permitting quantification of mean carbonyl content (gray) for each myofiber type. Morphometrics were determined from the sarcolemmal images of each fiber type. The white bar represents a length of 100 microns.

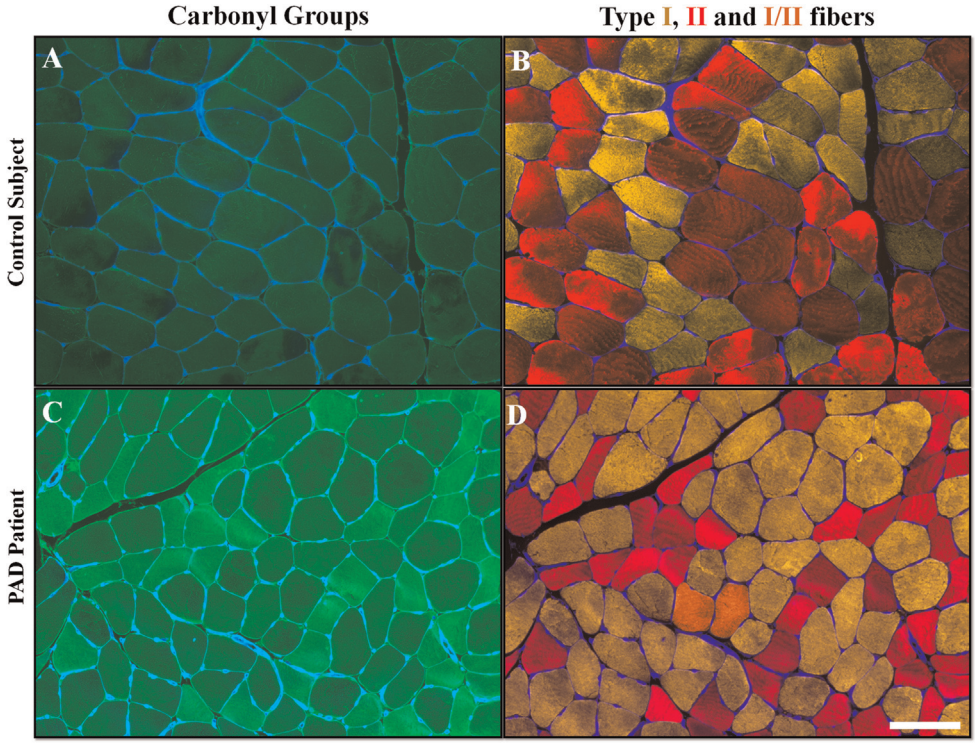

Fig. 3. Representative images of gastrocnemius specimens are from a control subject (A and B) and a PAD patient (C and D) (10x). Each muscle specimen was labeled for quantification of carbonyl content (A and C, green) and for identification of nuclei (blue nodes along the sarcolemma), sarcolemma (blue outlines) and Type I (yellow, B and D), Type II (red, B and D) and Type I/II (orange, D) myosin heavy chains. PAD myofibers exhibited higher carbonyl content as indicated by the brighter, green signal (compare A and C), a larger proportion of Type I fibers (yellow, compare B and D) and smaller cross-sectional area (compare B and D). Hybrid fibers contained both Type I and Type II myosin heavy chain (orange, D). The white bars represent a length of 100 μm.

Table 2
Carbonyl content and morphometric parameters of PAD and control gastrocnemius myofibers.

	Control	PAD	% Difference	p-value*
Type I	1137 ± 50	1424 ± 33	↑ 25	< 0.001
Type II	1175 ± 49	1578 ± 32	↑ 34	< 0.001
Type I/II	1251 ± 68	1601 ± 43	↑ 28	< 0.001
Combined	1216 ± 47	1519 ± 33	↑ 25	< 0.001
Cross-sectional area Type I	5748 ± 316	4154 ± 214	↓ 28	< 0.001
Cross-sectional area Type II	5692 ± 331	3408 ± 221	↓ 40	< 0.001
Cross-sectional area Type I/II	5550 ± 381	3538 ± 236	↓ 36	< 0.001
Combined	5642 ± 246	3700 ± 176	↓ 34	< 0.001
Equivalent diameter Type I	153 ± 5.4	134 ± 3.6	↓ 12	0.009
Equivalent diameter Type II	150 ± 6.1	117 ± 4.1	↓ 22	< 0.001
Equivalent diameter Type I/II	151 ± 6.8	121 ± 4.0	↓ 20	< 0.001
Combined	152 ± 4.6	124 ± 3.3	↓ 20	< 0.001
Perimeter Type I	626 ± 22	549 ± 15	↓ 12	0.009
Perimeter Type II	632 ± 24	500 ± 16	↓ 21	< 0.001
Perimeter Type I/II	616 ± 25	525 ± 15	↓ 15	0.004
Combined	626 ± 21	524 ± 12	↓ 16	< 0.001
Solidity Type I	0.941 ± 0.003	0.930 ± 0.002	↓ 1.2	0.009
Solidity Type II	0.935 ± 0.006	0.902 ± 0.004	↓ 3.5	< 0.001
Solidity Type I/II	0.892 ± 0.009	0.863 ± 0.006	↓ 3.2	0.004
Combined	0.923 ± 0.002	0.898 ± 0.003	↓ 2.7	< 0.001
Roundness Type I	0.630 ± 0.008	0.632 ± 0.005	↑ 0.3	0.793
Roundness Type II	0.632 ± 0.011	0.597 ± .008	↓ 5.5	0.015
Roundness Type I/II	0.554 ± 0.014	0.549 ± 0.009	↓ 0.9	0.756
Combined	0.609 ± 0.007	0.592 ± 0.006	↓ 2.8	0.094

* *p*-Values are adjusted for the effect of smoking status.

Gastrocnemius specimens of PAD patients exhibited increased oxidative damage, reduced myofiber size and altered morphology

Myofibers of PAD patients ($n=53$) exhibited a 25% greater burden of carbonyl groups (oxidative damage) (all myofiber types combined) compared to myofibers of control patients ($n=25$; Fig. 3). Furthermore, carbonyl content was significantly greater for each individual fiber Type in the PAD patients compared to controls (Table 2). In addition, almost every parameter of size and shape was significantly different in the myofibers (all myofiber types combined) of PAD patients compared to controls. This was also true for each individual Type of myofiber in PAD gastrocnemius compared to controls (Table 2).

Increased oxidative damage correlated inversely with the observed abnormalities in the size and shape of PAD myofibers, suggesting that increased oxidative damage produced loss of structural integrity of PAD myofibers. Specifically, the carbonyl content of PAD myofibers (all myofiber types combined) was negatively associated with myofiber cross-sectional area ($r=-0.401$, $p<0.001$), equivalent diameter ($r=-0.346$, $p=0.002$), perimeter ($r=-0.314$, $p=0.005$) and solidity ($r=-0.305$, $p=0.007$).

Type II and Type I/II (mixed) myofibers exhibited greater oxidative damage compared to Type I myofibers in PAD gastrocnemius

The variability of oxidative damage among myofibers in individual PAD and control specimens suggested the possibility of selective damage to the Type II fibers, previously shown to be preferentially affected in PAD muscle [3]. We found that oxidative damage was higher in Type II and Type I/II fibers compared to Type I fibers in PAD patients. Furthermore, Type II fibers demonstrated 34% increase (highest increase among the different myofiber types) of carbonyl content compared to control (Table 2). In PAD gastrocnemius, Type II and Type I/II fibers demonstrated greater damage compared to Type I (Type I *vs.* Type II, $p<0.001$; Type I *vs.* Type I/II, $p<0.001$). In the control gastrocnemius no differences were observed among the fiber types.

Type II and Type I/II (mixed) myofibers exhibited a greater reduction in size and alteration in shape compared to Type I myofibers in PAD gastrocnemius

Similar to the oxidative damage results, the parameters of myofiber size including cross-sectional area, equivalent diameter and perimeter and myofiber shape including solidity and roundness were significantly reduced in the PAD gastrocnemius myofibers compared to controls for all three myofiber types (Table 2).

Furthermore, in comparison to Type I myofibers, Type II fibers exhibited a greater decrease in cross-sectional area ($p<0.001$), equivalent diameter ($p<0.001$), perimeter ($p<0.001$), solidity ($p=0.020$) and roundness ($p=0.001$) (Table 3). Type I/II compared to Type I fibers exhibited decreased cross-sectional area ($p=0.002$), equivalent diameter ($p<0.001$), perimeter ($p=0.007$), and roundness ($p=0.019$) (Table 3). No differences were observed between Type II and Type I/II fibers.

Table 3
Carbonyl content and morphometric parameters in PAD-II and PAD-IV patients.

	PAD-II	PAD-IV	% Difference	p-value*
Type I	1329 ± 41	1496 ± 44	↑ 12	0.009
Type II	1493 ± 45	1643 ± 48	↑ 10	0.028
Type I/II	1483 ± 57	1701 ± 61	↑ 15	0.012
Combined	1435 ± 34	1613 ± 53	↑ 12	0.008
Cross-sectional area Type I	4747 ± 262	3497 ± 277	↓ 26	0.002
Cross-sectional area Type II	4294 ± 208	2519 ± 252	↓ 41	< 0.001
Cross-sectional area Type I/II	4523 ± 219	2453 ± 232	↓ 45	< 0.001
Combined	4521 ± 162	2823 ± 203	↓ 38	< 0.001
Equivalent diameter Type I	145 ± 4.2	122 ± 4.5	↓ 15	< 0.001
Equivalent diameter Type II	131 ± 4.6	99 ± 4.9	↓ 24	< 0.001
Equivalent diameter Type I/II	140 ± 4.1	98 ± 4.3	↓ 30	< 0.001
Combined	139 ± 3.1	107 ± 3.9	↓ 23	< 0.001
Perimeter Type I	586 ± 16	506 ± 17	↓ 14	0.002
Perimeter Type II	546 ± 18	443 ± 19	↓ 19	< 0.001
Perimeter Type I/II	605 ± 15	437 ± 15	↓ 28	< 0.001
Combined	579 ± 9.8	462 ± 14	↓ 20	< 0.001
Solidity Type I	0.938 ± 0.003	0.921 ± 0.003	↓ 1.8	< 0.001
Solidity Type II	0.918 ± 0.005	0.884 ± 0.005	↓ 3.7	< 0.001
Solidity Type I/II	0.861 ± 0.007	0.861 ± 0.008	0	0.981
Combined	0.905 ± 0.003	0.889 ± 0.004	↓ 1.8	0.003
Roundness Type I	0.645 ± 0.007	0.619 ± 0.007	↓ 4.0	0.013
Roundness Type II	0.624 ± 0.009	0.564 ± 0.010	↓ 9.6	< 0.001
Roundness Type I/II	0.552 ± 0.011	0.544 ± 0.011	↓ 1.4	0.609
Combined	0.606 ± 0.005	0.575 ± 0.008	↓ 5.1	0.004

* *p*-Values are adjusted for the effect of smoking status.

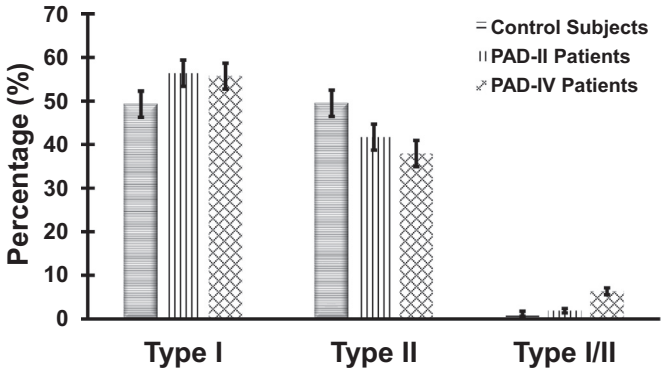

Fig. 4. Frequency of each fiber type in muscle from control subjects, PAD patients presenting with claudication (Fontaine stage II, PAD-II) and PAD patients presenting with critical limb ischemia (Fontaine stage IV, PAD-IV) is presented as percentage of all myofibers. The percentage of Type II fibers decreased while the percentage of Type I/II increased, as the disease progressed.

Oxidative damage increased in association with reduced myofiber size and altered myofiber morphometrics as the disease progressed

To evaluate the hypothesis that oxidative damage and myofiber size and shape are associated with the patient's stage of disease, we separated the PAD group (Table 1) into PAD Fontaine Stage II (Stage II, $n=28$ patients) and PAD Fontaine Stage IV (Stage IV, $n=25$ patients) and evaluated differences in myofiber oxidative damage and morphometrics in the gastrocnemius of the two groups (Table 3). Carbonyl content for all three fiber types was significantly increased in the PAD-IV patients compared to PAD-II patients (Table 3). Similarly, myofiber cross-sectional area, equivalent diameter, perimeter, solidity and roundness were significantly reduced in PAD-IV patients compared to PAD-II patients (Table 3). Among the myofibers of PAD-II patients, Type II fibers exhibited the most damage for all the parameters ($p < 0.01$) with the exception of solidity and roundness compared to Type I fibers. In contrast, in PAD-IV myofibers both Type II and Type I/II fibers were equally damaged compared to Type I fibers.

Type II fibers were preferentially lost, in PAD

Frequency analysis of Type I, Type II and Type I/II myofibers provided further support for our findings of selective oxidative damage to Type II myofibers with a shift in the ratio of Type II to Type I myofibers in PAD (Fig. 4). In the gastrocnemius of the control group, the proportion of Type I, Type II and transitional Type I/II fibers was 48%, 51% and 1%, respectively. In the gastrocnemius of PAD-II patients, the proportion of Type I, Type II and transitional Type I/II fibers was 56%, 42% and 2%, respectively. In PAD-IV patients the proportion of Type I, Type II and transitional Type I/II fibers was 56%, 38% and 6%, respectively. The data are consistent with a shift from Type II myofibers to Type I for both PAD groups ($p<0.01$) and indicate that with advancing disease there is a shift from Type II to Type I, transitioning through Type I/II.

Discussion

Our study of gastrocnemius muscle from patients with PAD demonstrates increased oxidative damage in all fiber types in the PAD patients compared to control subjects. Increased oxidative damage was associated with reduced size (decrease in cross-sectional area, equivalent diameter and perimeter) and abnormal shape (less polygonal and more irregular) of myofibers across all fiber types. Reports of preferential loss of Type II fibers in PAD skeletal muscle [3,9,15], led us to hypothesize that this loss is related to increased oxidative damage in Type II myofibers. In support of this hypothesis, our present study revealed greater oxidative damage in Type II compared to Type I myofibers in association with smaller fiber size and more pronounced abnormalities in fiber shape, changes that indicate significant damage to the myofibrillar, cytoskeletal and membranous components of the myofiber [16,17]. We also observed increased frequency, higher levels of oxidative damage and markedly altered size and shape of hybrid fibers (Type I/II) in PAD compared to control gastrocnemius. Hybrid fibers represent transitions between Type II and Type I fibers and become more numerous whenever fiber type shifts occur [18]. Therefore, the hybrid myofibers in PAD muscle are probably oxidatively damaged Type II myofibers transitioning to the Type I phenotype hence their higher carbonyl content, smaller size and increased frequency, with disease progression. In general, we found that for all myofiber types, oxidative damage, cross-sectional area and shape abnormalities are directly related to progression from claudication to tissue loss (critical limb ischemia). Taken together, our data demonstrate that in PAD, chronic ischemia and ischemia-reperfusion operate to increase oxidative damage that produces severe myopathic changes in the gastrocnemius muscle. The myopathy of PAD is characterized by preferential oxidative damage and degeneration of the fast twitch (Type II) myofibers and a fast (Type II) to slow (Type I) myofiber type shift represented by a decrease of Type II fibers and a concomitant increase of the Type I and mixed Type I/II fibers.

Muscle wasting is present in a variety of clinical conditions including disuse, denervation, microgravity, heart failure, chronic obstructive pulmonary disease, cachexia of cancer and sepsis and sarcopenia of aging [18,19]. In most of these conditions reduced myofiber size occurs preferentially in certain fiber types and/or is accompanied by shifts in the fiber type profile. Preferential reduction in the size of Type I fibers and a slow to fast myofiber shift is usually seen in the leg muscles of patients after disuse, denervation injury (nerve or spinal cord trauma), exposure to microgravity (space travel), heart failure or chronic obstructive pulmonary disease [18,19]. In contrast, a preferential reduction in the size of Type II fibers and a fast to slow shift is usually seen in the leg muscles of patients suffering from cancer, dietary insufficiency, sepsis and sarcopenia of aging [18,19]. Our findings suggest that the myopathy of PAD shares some similarities with the muscle wasting seen in diseases of nutrient-deficiency like cancer, sepsis and aging. This is potentially important for several reasons. First, it points to possible analogies between the mechanisms operating to produce the myopathy of PAD and those of cancer and aging [20–22]. Such mechanisms may (among others explored below) include a structural and dynamic malfunction of the vascular system in these diseases [23,24]. Second, it suggests that although decreased functional performance and activity is one of the prominent manifestations of PAD, it is unlikely that a disuse type of muscle wasting (usually seen with limb inactivity/immobilization or nerve injury) is a dominant contributor to the myopathy of PAD.

The mechanism of selective loss of Type II myofibers in PAD has not yet been established. Our results suggest that this loss is a consequence of selective oxidative damage to the Type II fibers (Fig. 4). To date, remarkably few investigations have been concerned with the biochemical basis for selective oxidative damage to and reduced size of Type II fibers in disease and aging. In a recent study of rat skeletal muscle, Anderson and Neufer [25] found a significantly higher mitochondrial free radical leak, expressed as the ratio of H_2O_2 production to O_2 utilization, in white (predominantly Type IIB fibers) and red (predominantly Type IIA fibers) gastrocnemius, compared to soleus muscle

(predominantly Type I fibers). They concluded that Type II fibers were potentiated uniquely to generation of H_2O_2. In a related study, Stefanyk et al. [26] identified a potential mechanism that could explain our present findings of fiber type selective oxidative damage and altered morphometrics. While studying fatty acid composition of mitochondrial membranes from soleus, red gastrocnemius and plantaris (predominantly Type IIB fibers) muscle of the rat, these investigators found a significantly higher mole fraction of saturated fatty acids and a lower mole fraction of ω6 polyunsaturated fatty acids in the soleus, compared to red gastrocnemius and plantaris. The unsaturation index and, therefore, the lipid peroxidation index were lower in the soleus. Similarly, cardiolipin of the mitochondrial membranes of the soleus contained more saturated fatty acids and less polyunsaturated fatty acids than the mitochondrial membranes of red gastrocnemius and plantaris, producing 20–30% lower unsaturation and lipid peroxidation indices in the soleus. Taken together, these findings are consistent with our present findings of increased sensitivity of II fibers to oxidative damage, leading to their preferential loss and a shift towards Type I myofibers in PAD.

A substantial body of work has explored the subject of muscle wasting and its relation to different acute or chronic diseases and aging and excellent reviews on the subject have been recently published [18,27]. At the molecular level certain common mechanisms appear to be related to preferential reduction in the size and frequency of Type II fibers in the nutrient-related (cancer, dietary insufficiency, sepsis and aging) type of muscle wasting. These mechanisms involve abnormal activation of the proteolytic pathways including the proteasomal and lysosomal pathways [28]. The best explored signaling networks involved in the process are related to the Forkhead box O family, the transforming growth factor beta family, and nuclear factor-kappaB [29–33]. Type II myofibers are more sensitive to these mechanisms and a significant factor contributing the resistance of Type I fibers is the activity of peroxisome proliferator-activated receptor gamma coactivator 1-alpha, a well described transcriptional coactivator required for mitochondrial biogenesis, protection from proteolysis and maintenance of the slow twitch, oxidative fiber phenotype of Type I myofibers [34–37].

This is a descriptive study and therefore its principal limitation is that it cannot establish cause and effect linkages between arterial blockages, oxidative damage, myofiber type degeneration and PAD clinical manifestations. Instead, the study demonstrated that there is increased oxidative damage in association with degeneration of myofiber size and shape in PAD gastrocnemius, that the damage is selective for Type II myofibers and is worse in the most advanced stage of PAD. These findings are in agreement with prior work from our and other laboratories demonstrating that arterial blockages in the legs of PAD patients produce ischemia-induced oxidative stress and progressive accumulation of oxidative damage to all the tissues (including muscle, nerves, skin, and subcutaneous tissues) of the affected limb [4,7,9,10,38,39]. In the long-term, this accumulation of oxidative damage in the ischemic tissues leads to gradual decline of the PAD limb and may contribute to progression of the manifestations of the disease from claudication to critical limb ischemia and eventual limb loss. Our findings are also consistent with the type of functional disability we see in PAD patients. Specifically, in PAD muscles Type II fibers that are high, energy consumers and are designed for short explosive movements appear to be preferentially lost while Type I fibers that are energy conserving and are optimized for prolonged low-intensity (fatigue resistant) activities are less damaged and more represented in the PAD muscle [40]. This selectivity may in part explain the fact that, compared to controls, PAD patients walk with reduced cadence, have decreased gait variability and decreased performance of the foot plantar flexors [41–43]. In this study, we evaluated oxidative damage in different myofiber types as a correlate of myofiber degeneration and PAD disease progression. In the future, more detailed evaluation of the proteolytic pathways and signaling networks responsible for myofiber degeneration and their Type II selectivity can be also evaluated in muscle samples obtained from PAD patients. High quality human data are critical for improving our knowledge of the mechanisms operating to produce PAD myopathy and for the development of specific therapies with validated biomarkers of relevance to underlying mechanisms. Several therapies including exercise, nutritional therapy, medications that enhance mitochondrial function and antioxidant defenses, androgens, growth hormone, ghrelin and its mimetics, myostatin inhibitors and anti-inflammatory agents have been proposed for the management of acquired myopathies [18,19] and may be promising approaches to the management of PAD patients.

In summary, our work demonstrates that there is increased myofiber oxidative damage and degeneration in PAD gastrocnemius, that this damage is selective for Type II myofibers and is worse in the most advanced stage of PAD. These findings are consistent with myofiber oxidative damage as a significant contributor to the pathophysiology of PAD and provide insight into possible mechanisms behind the preferential damage of Type II myofibers and the chronic and progressive nature of PAD. Accumulating oxidative damage in the ischemic limb may cause the patient to transition from claudication to critical limb ischemia and eventually limb loss. In the future this type of work can help identify the mechanisms responsible for the myopathy of PAD and can lead to a better understanding of the pathogenesis of the disease and to the design of individualized and targeted interventions essential for much needed improvement of diagnosis, staging and treatment of patients suffering from PAD.

Conflict of Interest

The authors declare no conflicts of interest.

Acknowledgments

This work was supported by NIH Grant R01AG034995, by the Charles and Mary Heider Fund for Excellence in Vascular Surgery, by the Alexander S. Onassis Public Benefit Foundation (grant no. F-ZD 036/2009-2010) and by the American Heart Association Pre-Doctoral Fellowship 13PRE13860010. Furthermore, this material is the result of work supported with resources and the use of facilities at the VA Nebraska and Western Iowa Health Care System.

References

[1] L.Norgren, W.R.Hiatt, J.A.Dormandy, M.R.Nehler, K.A.Harris, F.G.Fowkes, On behalf of the TASC II Working Group, Inter-society consensus for the management of peripheral arterial disease (TASC II), Journal of Vascular Surgery 45 (Suppl. S) (2007) S5–67. http://dx.doi.org/10.1016/j.redox.2014.07.002.

[2] K.Cluff, D.Miserlis, G.K.Naganathan, I.I.Pipinos, P.Koutakis, A.Samal, R.D. McComb, J.Subbiah, G.P.Casale, Morphometric analysis of gastrocnemius muscle biopsies from patients with peripheral arterial disease: Objective grading of muscle degeneration, American Journal of Physiology. Regulatory, Integrative and Comparative Physiology 305 (2013) R291–R299. http://dx.doi.org/10.1016/j.redox.2014.07.002 23720135.

[3] B.Hedberg, K.A.Angquist, K.Henriksson-Larsen, M.Sjöström, Fibre loss and distribution in skeletal muscle from patients with severe peripheral arterial insufficiency, European Journal of Vascular Surgery 3 (1989) 315–322. http://dx.doi.org/10.1016/j.redox.2014.07.002 2767254.

[4] I.I.Pipinos, A.R.Judge, J.T.Selsby, Z.Zhu, S.A.Swanson, A.A.Nella, S.L.Dodd, The myopathy of peripheral arterial occlusive disease: Part 2. Oxidative stress,

neuropathy, and shift in muscle fiber type, Vascular and Endovascular Surgery 42 (2008) 101–112. http://dx.doi.org/10.1016/j.redox.2014.07.002 18390972.
[5] I.I.Pipinos, A.R.Judge, Z.Zhu, J.T.Selsby, S.A.Swanson, J.M.Johanning, B.T.Baxter, T.G.Lynch, S.L.Dodd, Mitochondrial defects and oxidative damage in patients with peripheral arterial disease, Free Radical Biology & Medicine 41 (2006) 262–269. http://dx.doi.org/10.1016/j.redox.2014.07.002 16814106.
[6] I.I.Pipinos, S.A.Swanson, Z.Zhu, A.A.Nella, D.J.Weiss, T.L.Gutti, R.D.McComb, B.T. Baxter, T.G.Lynch, G.P.Casale, Chronically ischemic mouse skeletal muscle exhibits myopathy in association with mitochondrial dysfunction and oxidative damage, American Journal of Physiology. Regulatory, Integrative and Comparative Physiology 295 (2008) R290–R296. http://dx.doi.org/10.1016/j.redox.2014.07.002 18480238.
[7] I.I.Pipinos, A.R.Judge, J.T.Selsby, Z.Zhu, S.A.Swanson, A.A.Nella, S.L.Dodd, The myopathy of peripheral arterial occlusive disease: Part 1. Functional and histomorphological changes and evidence for mitochondrial dysfunction, Vascular and Endovascular Surgery 41 (2007) 481–489. http://dx.doi.org/10.1016/j.redox.2014.07.002 18166628.
[8] I.I.Pipinos, A.D.Shepard, P.V.Anagnostopoulos, A.Katsamouris, M.D.Boska, Phosphorus 31 nuclear magnetic resonance spectroscopy suggests a mitochondrial defect in claudicating skeletal muscle, Journal of Vascular Surgery 31 (2000) 944–952. http://dx.doi.org/10.1016/j.redox.2014.07.002 10805885.
[9] J.G.Regensteiner, E.E.Wolfel, E.P.Brass, M.R.Carry, S.P.Ringel, M.E.Hargarten, E.R. Stamm, W.R.Hiatt, Chronic changes in skeletal muscle histology and function in peripheral arterial disease, Circulation 87 (1993) 413–421. http://dx.doi.org/10.1016/j.redox.2014.07.002 8425290.
[10] D.J.Weiss, G.P.Casale, P.Koutakis, A.A.Nella, S.A.Swanson, Z.Zhu, D.Miserlis, J.M. Johanning, I.I.Pipinos, Oxidative damage and myofiber degeneration in the gastrocnemius of patients with peripheral arterial disease, Journal of Translational Medicine 11 (2013) 230. http://dx.doi.org/10.1016/j.redox.2014.07.002 24067235.
[11] N.A.Rubinstein, A.M.Kelly, Development of muscle fiber specialization, in: A. G. Engel, C. Franzini-Armstrong (Eds.), Myology, McGraw-Hill, New York, NY, USA, 2004, pp. 87–101.
[12] T.Hirao, M.Takahashi, Carbonylation of cornified envelopes in the stratum corneum, FEBS Letters 579 (2005) 6870–6874. http://dx.doi.org/10.1016/j.redox.2014.07.002 16336969.
[13] D.Huang, G.P.Casale, J.Tian, S.M.Lele, V.M.Pisarev, M.A.Simpson, G.P.Hemstreet3rd, UDP-glucose dehydrogenase as a novel field-specific candidate biomarker of prostate cancer, International Journal of Cancer 126 (2010) 315–327. http://dx.doi.org/10.1016/j.redox.2014.07.002.
[14] D.Huang, G.P.Casale, J.Tian, N.K.Wehbi, N.A.Abrahams, Z.Kaleem, L.M.Smith, S. L.Johansson, J.E.Elkahwaji, G.P.Hemstreet3rd, Quantitative fluorescence imaging analysis for cancer biomarker discovery: application to beta-catenin in archived prostate specimens, Cancer Epidemiology, Biomarkers & Prevention 16 (2007) 1371–1381. http://dx.doi.org/10.1016/j.redox.2014.07.002 17623804.
[15] B.Hedberg, K.A.Angquist, M.Sjöström, Peripheral arterial insufficiency and the fine structure of the gastrocnemius muscle, International Angiology: A Journal of the International Union of Angiology 7 (1988) 50–59 3385269.
[16] J.W.Sanger, J.Wang, Y.Fan, J.White, J.M.Sanger, Assembly and dynamics of myofibrils, Journal of Biomedicine & Biotechnology 2010 (2010) 858606. http://dx.doi.org/10.1016/j.redox.2014.07.002 20625425.
[17] J.W.Sanger, J.M.Sanger, C.Franzini-Armstrong, Assembly of the skeletal muscle cell, in: A.G. Engel, C. Franzini-Armstrong (Eds.), Myology, McGraw-Hill, New York, NY, USA, 2004, pp. 45–65.
[18] S.Ciciliot, A.C.Rossi, K.A.Dyar, B.Blaauw, S.Schiaffino, Muscle type and fiber type specificity in muscle wasting, International Journal of Biochemistry & Cell Biology 45 (2013) 2191–2199. http://dx.doi.org/10.1016/j.redox.2014.07.002 23702032.
[19] N.Johns, N.A.Stephens, K.C.H.Fearon, Muscle wasting in cancer, International Journal of Biochemistry & Cell Biology 45 (2013) 2215–2229. http://dx.doi.org/10.1016/j.redox.2014.07.002.
[20] Z.Ungvari, Z.Orosz, N.Labinskyy, A.Rivera, Z.Xiangmin, K.Smith, A.Csiszar, Increased mitochondrial H_2O_2 production promotes endothelial NF-kappaB activation in aged rat arteries, American Journal of Physiology. Heart and Circulatory Physiology 293 (2007) H37–H47. http://dx.doi.org/10.1016/j.redox.2014.07.002 17416599.
[21] Z.Ungvari, N.Labinskyy, S.Gupte, P.N.Chander, J.G.Edwards, A.Csiszar, Dysregulation of mitochondrial biogenesis in vascular endothelial and smooth muscle cells of aged rats, American Journal of Physiology. Heart and Circulatory Physiology 294 (2008) H2121–H2128. http://dx.doi.org/10.1016/j.redox.2014.07.002 18326800.
[22] A.J.Donato, A.Uberoi, D.W.Wray, S.Nishiyama, L.Lawrenson, R.S.Richardson, Differential effects of aging on limb blood flow in humans, American Journal of Physiology. Heart and Circulatory Physiology 290 (2006) H272–H278. http://dx.doi.org/10.1016/j.redox.2014.07.002 16183733.
[23] B.J.Behnke, M.D.Delp, P.J.Dougherty, T.I.Musch, D.C.Poole, Effects of aging on microvascular oxygen pressures in rat skeletal muscle, Respiratory Physiology & Neurobiology 146 (2005) 259–268. http://dx.doi.org/10.1016/j.redox.2014.07.002 15766914.
[24] J.A.Russell, C.A.Kindig, B.J.Behnke, D.C.Poole, T.I.Musch, Effects of aging on capillary geometry and hemodynamics in rat spinotrapezius muscle, American Journal of Physiology. Heart and Circulatory Physiology 285 (2003) H251–H258. http://dx.doi.org/10.1016/j.redox.2014.07.002 12649079.
[25] E.J.Anderson, P.D.Neufer, Type II skeletal myofibers possess unique properties that potentiate mitochondrial H(2)O(2) generation, American Journal of Physiology. Cell Physiology 290 (2006) C844–C851. http://dx.doi.org/10.1016/j.redox.2014.07.002 16251473.
[26] L.E.Stefanyk, N.Coverdale, B.D.Roy, S.J.Peters, P.J.LeBlanc, Skeletal muscle type comparison of subsarcolemmal mitochondrial membrane phospholipid fatty acid composition in rat, Journal of Membrane Biology 234 (2010) 207–215. http://dx.doi.org/10.1016/j.redox.2014.07.002 20336283.
[27] Y.Wang, J.E.Pessin, Mechanisms for fiber-type specificity of skeletal muscle atrophy, Current Opinion in Clinical Nutrition and Metabolic Care 16 (2013) 243–250. http://dx.doi.org/10.1016/j.redox.2014.07.002 23493017.
[28] S.Schiaffino, K.A.Dyar, S.Ciciliot, B.Blaauw, M.Sandri, Mechanisms regulating skeletal muscle growth and atrophy, FEBS Journal 280 (2013) 4294–4314. http://dx.doi.org/10.1016/j.redox.2014.07.002 23517348.
[29] Z.Huang, X.Chen, D.Chen, Myostatin: A novel insight into its role in metabolism, signal pathways, and expression regulation, Cellular Signalling 23 (2011) 1441–1446. http://dx.doi.org/10.1016/j.redox.2014.07.002 21609762.
[30] D.Cai, J.D.Frantz, N.E.TawaJr., P.A.Melendez, B.C.Oh, H.G.Lidov, P.O.Hasselgren, W.R.Frontera, J.Lee, D.J.Glass, S.E.Shoelson, IKKβ/NF-κB activation causes severe muscle wasting in mice, Cell 119 (2004) 285–298. http://dx.doi.org/10.1016/j.redox.2014.07.002 15479644.
[31] C.L.Mendias, J.P.Gumucio, M.E.Davis, C.W.Bromley, C.S.Davis, S.V.Brooks, Transforming growth factor-beta induces skeletal muscle atrophy and fibrosis through the induction of atrogin-1 and scleraxis, Muscle & Nerve 45 (2012) 55–59. http://dx.doi.org/10.1016/j.redox.2014.07.002 22190307.
[32] M.Sandri, C.Sandri, A.Gilbert, C.Skurk, E.Calabria, A.Picard, K.Walsh, S.Schiaffino, S.H.Lecker, A.L.Goldberg, Foxo transcription factors induce the atrophy-related ubiquitin ligase atrogin-1 and cause skeletal muscle atrophy, Cell 117 (2004) 399–412. http://dx.doi.org/10.1016/j.redox.2014.07.002 15109499.
[33] C.Mammucari, G.Milan, V.Romanello, E.Masiero, R.Rudolf, P.Del Piccolo, S.J. Burden, R.Di Lisi, C.Sandri, J.Zhao, A.L.Goldberg, S.Schiaffino, M.Sandri, FoxO3 controls autophagy in skeletal muscle in vivo, Cell Metabolism 6 (2007) 458–471. http://dx.doi.org/10.1016/j.redox.2014.07.002 18054315.
[34] J.T.Selsby, K.J.Morine, K.Pendrak, E.R.Barton, H.L.Sweeney, Rescue of dystrophic skeletal muscle by PGC-1alpha involves a fast to slow fiber type shift in the mdx mouse, PloS One 7 (2012) e30063. http://dx.doi.org/10.1016/j.redox.2014.07.002 22253880.
[35] M.Sandri, J.Lin, C.Handschin, W.Yang, Z.P.Arany, S.H.Lecker, A.L.Goldberg, B.M. Spiegelman, PGC-1alpha protects skeletal muscle from atrophy by suppressing FoxO3 action and atrophy-specific gene transcription, Proceedings of the National Academy of Sciences of the United States of America 103 (2006) 16260–16265. http://dx.doi.org/10.1016/j.redox.2014.07.002 17053067.
[36] S.Takikita, C.Schreiner, R.Baum, T.Xie, E.Ralston, P.H.Plotz, N.Raben, Fiber type conversion by PGC-1alpha activates lysosomal and autophagosomal biogenesis in both unaffected and Pompe skeletal muscle, PloS One 5 (2010) e15239. http://dx.doi.org/10.1016/j.redox.2014.07.002 21179212.
[37] S.S.Wing, S.H.Lecker, R.T.Jagoe, Proteolysis in illness-associated skeletal muscle atrophy: From pathways to networks, Critical Reviews in Clinical Laboratory Sciences 48 (2011) 49–70. http://dx.doi.org/10.1016/j.redox.2014.07.002 21699435.
[38] E.P.Brass, W.R.Hiatt, A.W.Gardner, C.L.Hoppel, Decreased NADH dehydrogenase and ubiquinol–cytochrome c oxidoreductase in peripheral arterial disease, American Journal of Physiology. Heart and Circulatory Physiology 280 (2001) H603–H609 11158957.
[39] K.I.Makris, A.A.Nella, Z.Zhu, S.A.Swanson, G.P.Casale, T.L.Gutti, A.R.Judge, I.I. Pipinos, Mitochondriopathy of peripheral arterial disease, Vascular 15 (2007) 336–343. http://dx.doi.org/10.1016/j.redox.2014.07.002 18053417.
[40] N.A.Rubinstein, A.M.Kelly, Development of muscle fiber specialization in the rat hindlimb, Journal of Cell Biology 90 (1981) 128–144. http://dx.doi.org/10.1016/j.redox.2014.07.002 7251670.
[41] P.Koutakis, J.M.Johanning, G.R.Haynatzki, S.A.Myers, N.Stergiou, G.M.Longo, I.I. Pipinos, Abnormal joint powers before and after the onset of claudication symptoms, Journal of Vascular Surgery 52 (2010) 340–347. http://dx.doi.org/10.1016/j.redox.2014.07.002 20670775.
[42] P.Koutakis, I.I.Pipinos, S.A.Myers, N.Stergiou, T.G.Lynch, J.M.Johanning, Joint torques and powers are reduced during ambulation for both limbs in patients with unilateral claudication, Journal of Vascular Surgery 51 (2010) 80–88. http://dx.doi.org/10.1016/j.redox.2014.07.002 19837536.
[43] S.A.Myers, J.M.Johanning, N.Stergiou, R.I.Celis, L.Robinson, I.I.Pipinos, Gait variability is altered in patients with peripheral arterial disease, Journal of Vascular Surgery 49 (2009) 924–931. http://dx.doi.org/10.1016/j.redox.2014.07.002 19217749.